MJFAS MALAYSIAN JOURNAL OF FUNDAMENTAL AND APPLIED SCIENCES
PRINT ISSN: 2289-5981 | ONLINE ISSN: 2289-599X

RESEARCH ARTICLE

Synthesis of carbon self-doped titanium dioxide and its activity in the photocatalytic oxidation of styrene under visible light irradiation

Siti Hajar Alias [a, b], Nurul Najidah Mohamed [a], Leaw Wai Loon [c], Sheela Chandren [a, c,*]

[a] *Department of Chemistry, Faculty of Science, Universiti Teknologi Malaysia, 81310 UTM Johor Bahru, Johor, Malaysia*
[b] *Faculty of Applied Sciences, Universiti Teknologi MARA Perlis, 02600 Arau, Perlis, Malaysia*
[c] *Centre for Sustainable Nanomaterials, Ibnu Sina Institute for Scientific and Industrial Research, Universiti Teknologi Malaysia, Skudai 81310, Johor, Malaysia*

* *Corresponding author: sheela@utm.my*

Article history
Received 20 February 2019
Revised 6 March 2019
Accepted 27 March 2019
Published Online 14 April 2019

Graphical abstract

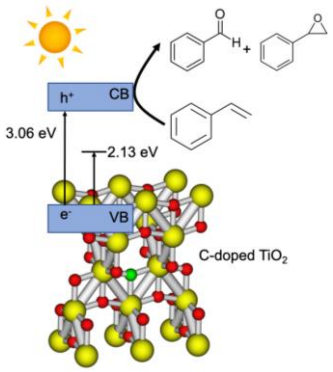

Abstract

Carbon self-doped titanium dioxide (C/TiO_2) photocatalyst was synthesized by a simple sol-gel method using titanium isopropoxide as both the titanium precursor and carbon source. The effects of calcination temperatures in the range of 300 to 700 °C to the structure and physicochemical properties of the C/TiO_2 were investigated by X-ray diffraction (XRD), field emission scanning electron microscopy (FESEM) coupled with energy dispersive X-ray (EDX), Fourier transform infrared (FTIR) spectroscopy, UV-visible diffuse reflectance (UV-Vis DR) spectroscopy, photoluminescence spectroscopy, N_2 adsorption-desorption and X-ray photoelectron spectroscopy (XPS). XPS results proved the presence of self-doped carbon at the interstitial and substitutional lattice of TiO_2. The C/TiO_2 calcined at 300 and 400 °C (C/TiO_2-300 and C/TiO_2-400, respectively) showed mesoporous characteristic and large surface area of about 100 $m^2\ g^{-1}$. The C/TiO_2 photocatalysts were then tested in the photo-oxidation of styrene under visible light irradiation with aqueous hydrogen peroxide as the oxidizing agent. The C/TiO_2 photocatalysts were successfully activated under the irradiation of visible light, where C/TiO_2-300 and C/TiO_2-400 showed the highest total concentration of products (benzaldehyde and styrene oxide) at 1.1 mmol and 1.0 mmol, respectively.

Keywords: Titanium dioxide, carbon doped, photocatalytic activity, styrene, photo-oxidation

INTRODUCTION

Titanium dioxide (TiO_2) is considered to be an excellent and superior photocatalytic material due to its low material cost, excellent stability, high specific surface area, environmental friendliness, nontoxicity, and superior photocatalytic activity (Ganesan *et al.*, 2015, Lavand and Malghe, 2015). Despite its numerous advantages, two significant drawbacks have hindered the usage of TiO_2 in further applications. The first drawback is that the band gap of anatase TiO_2 is fairly large, at about 3.20 eV, and can only be activated under UV light irradiation in the solar spectrum. However, UV light only constitutes to a small fraction (3-5%) of the solar spectrum (Hamal and Klabunde, 2007). In order to utilize free and abundance solar energy, more researches should be focused on visible light driven photocatalyst since visible light covers about 39% of the sunlight rays. The second drawback is the fast electron-hole pair recombination, an undesirable process where the absorbed energy is wasted as heat or reemitted without doing any chemical work. These two inherent properties are the major reasons for the low efficiency and are obstacles for practical applications of TiO_2. Therefore, in order to establish an economical, safe and clean reaction system, researchers are digging into suitable methods to modify TiO_2 to enhance its photocatalytic performance.

The addition of small amounts of carbon impurity to TiO_2 semiconductor, or referred as C-doped TiO_2, is one of the best methods to improve the photocatalytic performance under visible light irradiation. In the past decade, C-doped TiO_2 (C/TiO_2) has been synthesized by a variety of methods including thermal plasma (Park *et al.*, 2010), xerogel carbonization (Liu *et al.*, 2014), hydrothermal (Parayil *et al.*, 2012) and sol-gel methods (Liu *et al.*, 2012).

Most of the synthesis of pure TiO_2 in previous studies are focused on the application in UV light, such as the photocatalytic degradation of organic pollutants under UV light irradiation. One of the simplest method in synthesizing pure TiO_2 is by using titanium alkoxide as the titanium precursor. Titanium alkoxide will be hydrolyzed and the polycondensations of metal alkoxides, leading to the formation of extended network (Simonsen and Søgaard, 2010). The TiO_2 formed might contain a small amount of C doped inside the lattice of TiO_2 as a result of incomplete hydrolyzation of the titanium alkoxide. This formation of self-doped C could be responsible in enhancing the photocatalytic activity in the visible light region (Lettmann *et al.*, 2001).

The photo-oxidation of styrene are of great interest at academic and commercial levels. The oxidation of styrene produces benzaldehyde, styrene oxide and phenylacetaldehyde, which are useful intermediates in the fine chemicals and pharmaceuticals industry. A few studies

attempted to explain the formation of C self-doped TiO_2. Park and Luna synthesized C self-doped TiO_2 by hydrolysis of titanium butoxide, without using any external precursor and the obtained material was used in the photocatalytic reaction of 4-chlorophenol and acetominophen (Park *et al.*, 2009, Luna *et al.*, 2016). In another research, Gorska and coworkers (Gorska *et al.*, 2009) reported the synthesis of C self-doped TiO_2 by the hydrolysis of titanium (IV) isopropoxide for the degradation of phenol. However, to the best of our knowledge, research publications based on the synthesis and application of C self-doped TiO_2 (C/TiO_2) in the photo-oxidation of styrene under the irradiation of visible light.

Therefore, in this study, the photocatalytic capability of C self-doped TiO_2 photocatalyst in visible light is shown through the photocatalytic oxidation of styrene with hydrogen peroxide (H_2O_2) as the oxidizing agent. The presence self-doped C and its relation to the photocatalytic activity of TiO_2 with increasing calcination temperature are investigated and studied in details.

EXPERIMENTAL

Materials

The chemicals used in the synthesis of C self-doped TiO_2 were isopropyl alcohol (i-PrOH, 99.8%, Qrec), ethanol (EtOH, 95%, VChem), and titanium tetraisopropoxide (TTIP, 97%, Sigma-Aldrich). Meanwhile, the chemicals used for the photo-oxidation reaction were styrene (99%, Merck), acetonitrile (reagent grade, Merck), and hydrogen peroxide (30%, Merck). As for the standard in the photo-oxidation of styrene, the chemicals used were benzaldehyde (99% Aldrich) and styrene oxide (97%, Aldrich). Commercial TiO_2 was purchased from ACROS (98%).

Synthesis of C self-doped TiO_2 photocatalyst

20 mL of ethanol and 80 mL of deionized water were mixed to form a mixture. 6 mL of titanium tetraisopropoxide (TTIP) were then added drop-wise into the mixture to form a white precipitate. The mixture was kept under constant stirring at room temperature for 24 hours. Following that, it was then centrifuged, washed and dried at 80 °C for 5 hours, to obtain C/TiO_2. Finally, the synthesized C/TiO_2 were calcined at temperatures of 300, 400, 500, 600 and 700 °C for 5 hours. The samples are denoted as C/TiO_2-X, where X stands for the calcination temperature that was used to prepare it.

Characterization

The physicochemical properties of C/TiO_2 were determined by various characterization techniques. The crystalline phase and crystallite size of the C/TiO_2 were determined by X-ray diffractometer (Bruker AXS D8 Automatic Powder Diffractometer) operating at 40 kV, 30 mA and Cu Kα radiation ($\lambda = 1.5406$ nm) at $2\theta = 10 - 90$ °. The surface morphology of C/TiO_2 and commercial TiO_2 were observed from the magnified images of the crystallites by field-emission scanning electron microscopy (FESEM). The weight percentage of atoms on the sample surface was observed by energy dispersive X-ray (EDX) analysis. The sample was scanned with parameters i.e. accelerating voltage of 15.0 kV, probe current of 2.56160 nA and the range energy of 0 - 20 keV. Fourier transform infrared (FTIR) spectroscopy (Nicolet 6700 Thermo Scientific Infrared Spectrophotometer) was used to detect the existence of C group and other functional groups of the samples in TiO_2. For the UV-visible diffuse reflectance (UV-Vis DR) spectroscopy, a Perkin Elmer Lambda 35 UV-Vis-NIR spectrometer was used. The spectra were recorded at room temperature in air at a wavelength range of 200 to 800 nm. The photoluminescence analysis was done in order to study the electrons-holes recombination of the photocatalysts. Emission spectra of the samples were determined at room temperature using JASCO spectrofluorometer (FP-8500) with 150 W Xe lamp as the source of excitation. The sample excitation was conducted at 355 nm and the emission was scanned from 200 to 800 nm. The specific surface area and the type of porosity of the samples were assessed from Brunauer-Emmett-Teller (BET) analysis by measurement of nitrogen adsorption-desorption (Quantachrome NOVA touch LX4) at multilevel as a function of relative pressure. The relative pressure P/P_0 (P and P_0 are the pressure of N_2 vapour and its saturation vapour pressure at 77 K, respectively) used in the calculation of BET surface area. The data was automatically recorded into the computer. By using the model of Barrett-Joyner-Halenda (BJH), the pore volume and pore size distribution were calculated from the desorption branch. The X-ray photoelectron spectra (XPS) were recorded using high resolution multi technique X-ray spectrometer (Axis Ultra DLD XPS, Kratos). The binding energy of C1s at 285 eV was used as the internal reference to calibrate all the binding energies. Density functional theory (DFT) by Gaussian 09 sofware was used to detect the presence of the sub-band gap energy induced by the self-doped C is further proved by computing the band gap energy of anatase.

Photocatalytic oxidation of styrene

The photocatalytic activity of C/TiO_2 photocatalysts were tested by the photo-oxidation of styrene under visible light irradiation. The reaction mixture of styrene (10 mmol), 30% aqueous H_2O_2 (10 mmol) as the oxidizing agent, acetonitrile (5 mL) as the solvent and catalyst (50 mg), were placed in a capped-glass tube. The reactions were performed under visible light irradiation at room temperature for 24 hours. The type of lamp used as visible light source was halogen lamp with the power of 150 W. The reactions were placed at a distance of 10 cm from the light source and magnetically stirred throughout the irradiation. The blank reaction was also carried out in same condition but without catalyst. After 24 hours, the catalyst and products were separated from the mixture by centrifugation.

Gas chromatography-flame ionization detector (GC-FID) (Shimadzu GC-2014) with non-polar capillary column (BPX5) was used to identify the reaction product of styrene oxidation. A column flow of 3 mL/min with nitrogen and hydrogen as carrier gas were used. Operating conditions of GC-FID were as follows: oven temperature of 80 °C; initial temperature of 80 °C; initial time of 1 min; final temperature of 140 °C; hold time of 0.5 min; rate of 15 °C min^{-1}. Standards of products (benzaldehyde and styrene oxide) were prepared with acetonitrile as the solvent in order to obtain the calibration curve and allow the identification of products. The concentration of products (mmol) was calculated using the equation obtained from the calibration curve graph.

RESULTS AND DISCUSSION

Physicochemical properties of C/TiO_2 at different calcination temperatures

The presence of the self-doped carbon in the TiO_2 lattice has been proven by the analyses of EDX, FTIR and XPS. Table 1 shows the elemental composition of C/TiO_2 determined by EDX. The results confirmed the presence of Ti, O and C as the main elements in C/TiO_2. As compared to commercial TiO_2, the carbon composition for C/TiO_2 shows higher amount of self-doped carbon incorporated into TiO_2 lattice. With the increase of calcination temperature, the amount of carbon in C/TiO_2 were decreased as carbon was decomposed during the calcination process.

Fig. 1 shows the FTIR spectra for C/TiO_2 photocatalyts at calcination temperatures of 300, 400, 500, 600, and 700 °C. For C/TiO_2, a weak adsorption peak observed in C/TiO_2 at the wavelength of 1664-1707 and 1260-1000 cm^{-1}, which are attributed to the stretching vibrations of C=O and C–O, respectively. The observation of these peaks further proved the presence of self-doped carbon into TiO_2 lattice of C/TiO_2. A broad adsorption peak at 3000-3500 cm^{-1} and the adsorption peak at 1630 cm^{-1} in both C/TiO_2 and commercial TiO_2 were assigned to the surface hydroxyl groups (Kumar *et al.*, 2000). It was observed that when the calcination increased to high temperature, these hydroxyl peaks were decreased and reduced significantly. In addition, the broad peak observed at around 450-890 cm^{-1} corresponded to the Ti–O bond.

XPS measurements were carried out to determine the concentrations of carbon and their chemical states. The XPS survey spectra in Fig. 2 (a) confirmed the existence of Ti, O and C elements in C/TiO_2 and the atomic concentration of the elements are tabulated in Table 1. The atomic percentage of carbon element decreased with increasing calcination temperature.

Table 1 Summary of the physicochemical properties of the commercial TiO_2 and synthesized C/TiO_2.

Samples	Crystallite Size (nm)[a]	Atomic Weight[b] (%)			Atomic Concentration[c] (%)			Band Gap[d] (eV)	Surface Area[e] (m^2/g)	Pore Volume[f] (cm^3/g)	Pore Diameter[f] (nm)
		Ti	O	C	Ti	O	C				
Commercial	26.26	55.5	39.6	4.9	21	47	32	3.44	11	N/A	N/A
C/TiO_2-300	5.52	51.3	40.6	8.1	-	-	-	3.54	150	0.32	4.6
C/TiO_2-400	6.99	-	-	-	-	-	-	3.56	116	0.28	5.4
C/TiO_2-500	12.11	-	-	-	21	49	30	3.49	64	0.14	6.3
C/TiO_2-600	28.20	-	-	-	-	-	-	3.21	12	0.03	8.1
C/TiO_2-700	28.75	57.2	35.0	7.7	29	53	18	3.13	7	N/A	N/A

[a] Calculated by Scherrer equation. [b] Detemined from the EDX analysis. [c] Calculated from XPS spectra. [d] Optical band edge from Tauc plot of UV absorption studies. [e] BET surface area calculated from the linear part of the BET plot. [f] Calculated from BJH distribution

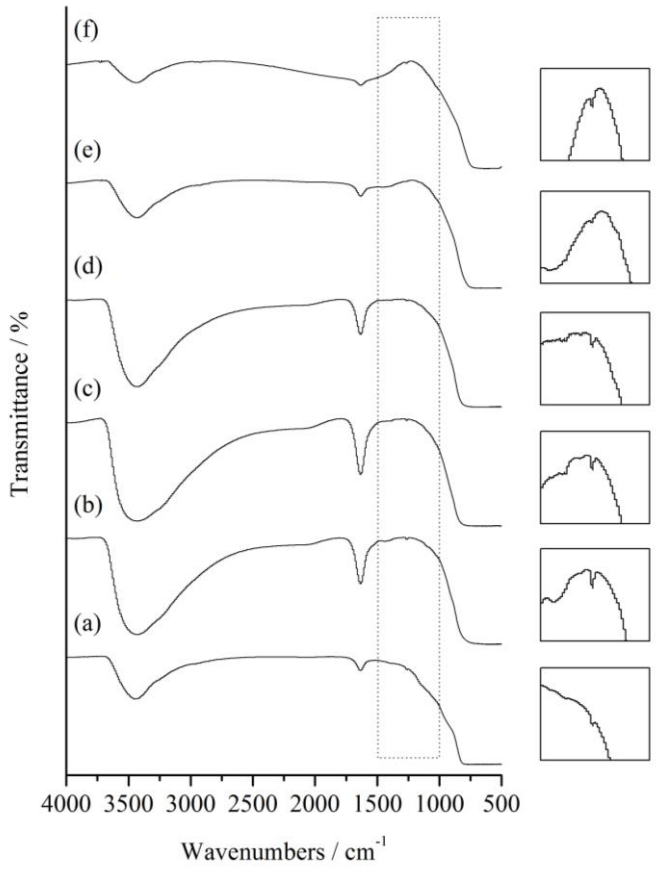

Fig. 1 FTIR spectra of (a) commercial TiO_2 and C/TiO_2 samples at different calcination temperatures of (b) 300, (c) 400, (d) 500, (e) 600, and (f) 700 °C. The insets show a zoomed plot of the adsorption peak at 1500-1000 cm^{-1}, which corresponds to C–O stretching vibrations.

This is in well agreement with the EDX and FTIR results. Meanwhile, Fig. 2 (b) to (d) show the high resolution XPS spectra of Ti 2p, O 1s and C 1s for C/TiO_2-500, C/TiO_2-700 and commercial TiO_2. In the Ti 2p spectra (Fig. 2 (b)), two peaks that appeared at 459 and 465 eV for all of spectra were the typical peaks of Ti $2p_{3/2}$ and Ti $2p_{1/2}$ binding energy region (Choi *et al.*, 2004, Shao *et al.*, 2010). This indicates the presence of Ti^{4+} ions in TiO_2 (Parayil *et al.*, 2012).The slight shifting in C/TiO_2 peaks from calcination temperature of 500 to 700 °C was due to the change in the bonding environment of Ti when calcination temperature increased. For C/TiO_2 calcined at 700 °C and the commercial TiO_2, beside Ti $2p_{3/2}$ binding energy of Ti^{4+}, a new and weak Ti $2p_{3/2}$ core level peak appeared around 456-457.4 eV, suggesting that Ti^{3+} species were formed in the TiO_2 lattice due to the partial reduction of Ti^{4+} to Ti^{3+}. The emergence of Ti^{3+} species would result in the formation of oxygen vacancy defects due to C-doping which took place during the synthesis of the catalysts (Raja *et al.*, 2006, Shao *et al.*, 2010).

Fig. 2 (c) displays spectra corresponding to O1s region for, C/TiO_2-500, C/TiO_2-700 and commercial TiO_2. All samples exhibited strong peaks at around 530 eV, which is the result of Ti–O bonds and the peak around 532 eV is due to the presence of C–O bond. In C/TiO_2-500 and commercial TiO_2, a signal at around 533 eV was detected due to the presence of C=O bond. An additional peak at around 527.7-529.1 eV for all the samples is possibly attributed to the presence of O atoms bonded with Ti^{3+} (Kumar *et al.*, 2000, Shao *et al.*, 2010). Ti^{3+} ions could act as an electron trap in the photocatalytic reaction and thus preventing the recombination of the charge carriers (Muniandy *et al.*, 2016).

Fig. 2 (d) compares the XPS profiles in the region of C1s binding energy for C/TiO_2-500, C/TiO_2-700 and commercial TiO_2. In all of the spectra, the peak attributed to C1s was observed in the range of 290 to 282 eV with two to four of deconvulated peaks. The peak signal at around 285 eV for all of the samples corresponds to the C–C and C–H bonds due to the presence of elemental carbon (sp^2 hybridized carbon) as well as adventitious carbon (Yang *et al.*, 2008, Lim *et al.*, 2010, Shao *et al.*, 2010, Muniandy *et al.*, 2016). The peak around 283 eV corresponded to the Ti–C bond due to the substitutional of C atom to O in TiO_2 lattice (Shao *et al.*, 2010). All spectra have a peak signal around 289 eV that corresponds to the O=C–O bond and an additional peak in C/TiO_2-500 at 287 eV, corresponding to C–O bond (Muniandy *et al.*, 2016). The presence of the carbonate-like species, O=C–O and C–O bond were due to interstitial and/or substitutional C to Ti atom in TiO_2 lattice (Liu *et al.*, 2014, Muniandy *et al.*, 2016). The presence of these three peaks indicate that C was self-doped into TiO_2's lattice at substitutional and interstial positions.

Photoluminescence (PL) study was conducted in order to understand the nature of the electron-hole recombination of the composites. In the field of photocatalysis, it is a good technique to understand the separation efficiency of photogenerated electrons and holes. Fig. 3 illustrates the PL spectra obtained from the recombination of electrons and holes for C/TiO_2 calcined at 300, 400, 500, 600 and 700 °C, and commercial TiO_2 in the range of 340 - 600 nm with 325 nm wavelength excitation source. The PL spectra displayed a similar pattern with three main peaks observed at 337-340 nm, 362-364 nm and 408-413 nm. The intense peak observed at 337-340 nm is assigned to the band luminescence the samples. Peaks at 362-364 nm and 408-413 nm arise from recombination at dopant levels or sub-band gaps induced by self-doped C and oxygen vacancies (Kavitha and Devi, 2014). Meanwhile, the small emission peak at 468 nm is due to the surface oxygen vacancies when Ti^{3+} charge is transferred to oxygen vacancy in TiO_6^{8-} octahedra (Kavitha and Devi, 2014, Kao and Chen, 2017).

The presence of the sub-band gap energy induced by the self-doped C is further proved by computing the band gap energy of anatase using density functional theory (DFT) as shown in Fig. 4. DFT calculations of 51 atoms (2×1×1 supercell) of $Ti_{21}O_{30}$ anatase cluster were performed using Gaussian 09 sofware. The C-doped was studied at substitutional position (by replacing oxygen) and interstitial position. The doping concentration of C at substitutional and interstial position is 1.96 at.% and 1.92 at.%, respectively. The calculated results shows that by doping with C, additional energy levels were formed in the band gap of anatase called sub-band gap at 2.13 eV for substitutional and 2.77 eV at interstitial position, which is in the visible light region (Siti Hajar Alias, 2019).

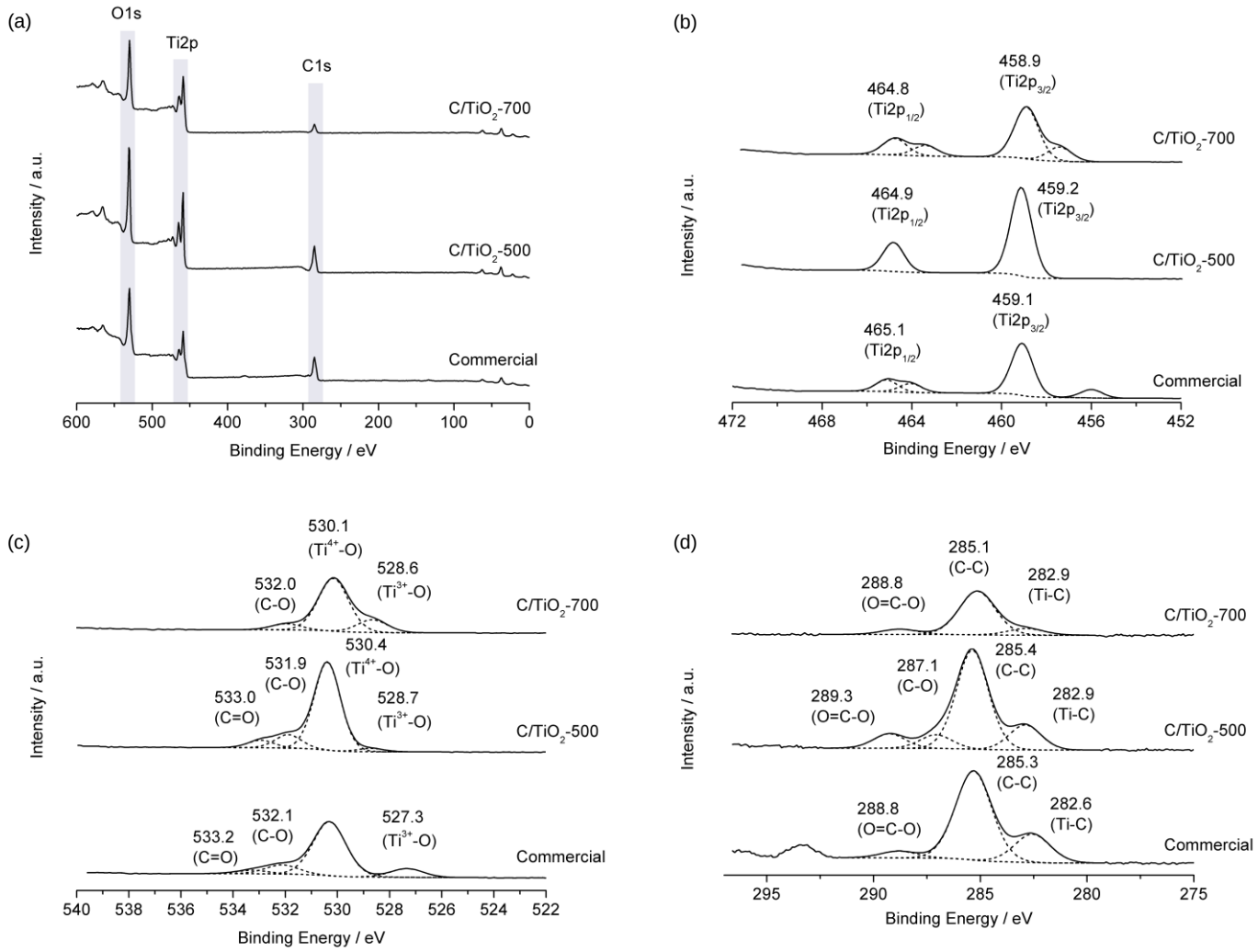

Fig. 2 (a) XPS survey specta and the binding energy of (b) Ti2p, (c) O1s and (d) C1s of commercial TiO_2, C/TiO_2-500, and C/TiO_2-700.

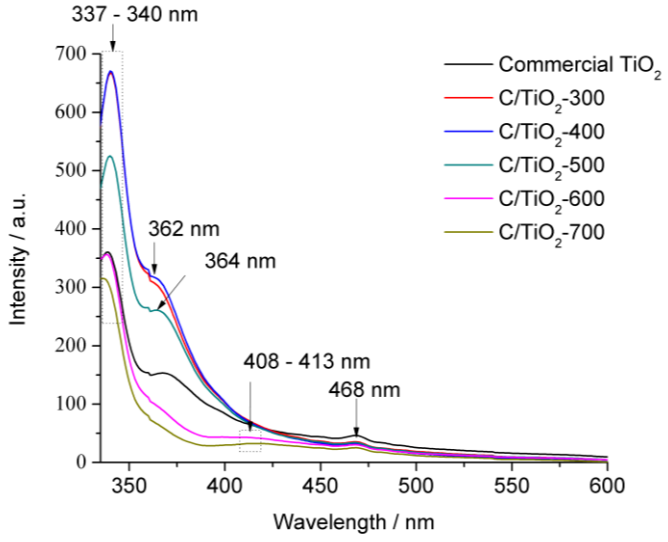

Fig. 3 Photoluminescence spectra of (a) commercial TiO_2 and (b) /TiO_2 samples at different calcination temperature (b) 300, (c) 400, (d) 500, (e) 600, and (f) 700 °C.

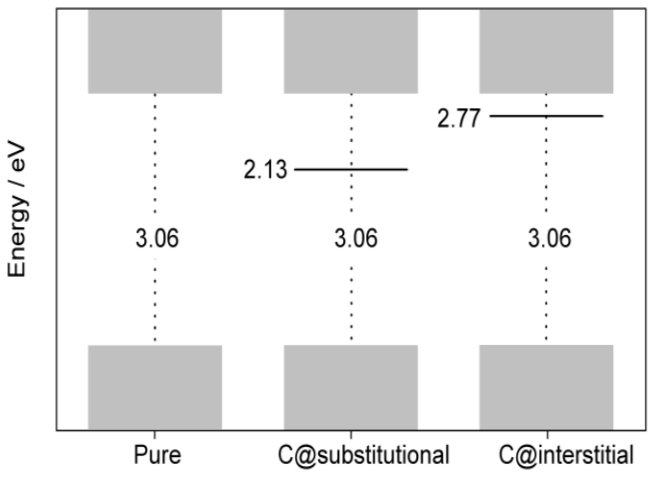

Fig. 4 Schematic illustration of the band gap energy of pure anatase $Ti_{21}O_{30}$, C-doped at substitutional position and C-doped at interstial position of anatase $Ti_{21}O_{30}$ calculated by DFT.

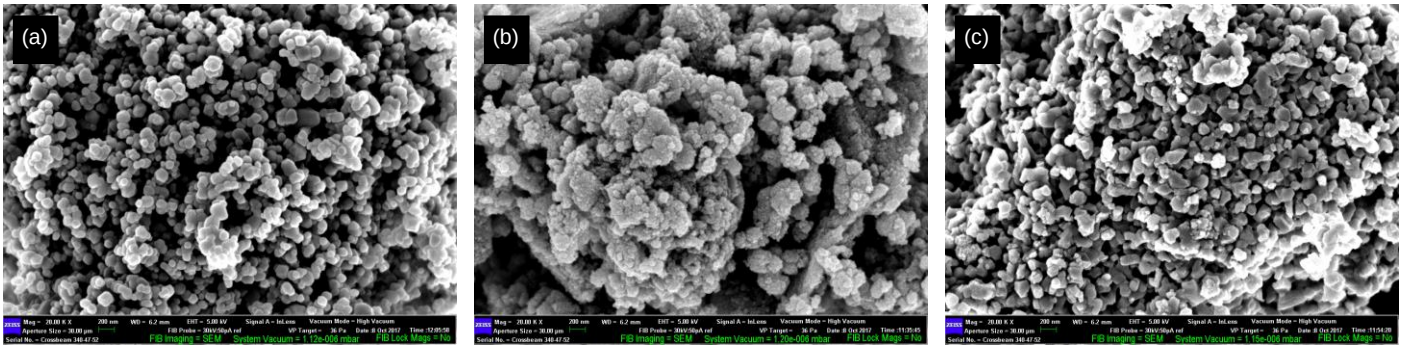

Fig. 6 FESEM images of (a) commercial TiO_2, (b) C/TiO_2-300, and (c) C/TiO_2-700 composites.

Fig. 5 (a) shows the XRD pattern of commercial TiO_2 anatase. It was observed that the sharp features of the XRD pattern is consistent with the anatase phase. Fig. 5 (b) to (f) shows the effect of calcination temperatures to the phase structures of C/TiO_2. From the results, it can be seen that the calcination temperature strongly influenced the phase composition and crystallinity of the TiO_2. As shown in Fig. 5, the C/TiO_2 photocatalyst was in the anatase phase with calcination temperature of 300 to 500 °C (JCPDS No. 21-1272), with the diffraction peaks observed at 2θ values of 25.3° and 48°. As the calcination temperature increased to 600 °C, the phase transformed to rutile phase with the composition of 43.45%. Upon increasing the calcination temperature to 700 °C, the anatase phase was mostly transformed into highly organized rutile phase by reconstruction of the TiO_6 octahedral (Hanaor and Sorrell, 2011). The diffraction peaks located at 2θ values of 27.4°, 36.1°, 41.2°, 54.3° and 56.6° were attributed to the rutile phase of TiO_2 (JCPDS No. 21-1276). The smallest crystallite sizes are obtained from C/TiO_2-300 and it increased from 5.52 to 28.75 nm, when the calcination temperature increased to 700 °C, as shown in Table 1. As the calcination temperature increase, the former crystallites also increased, which can be ascribed to the thermally promoted crystalline growth.

The FESEM image of the commercial TiO_2 is presented in Fig. 6 (a). It shows that the morphology of the commercial TiO_2 is spherical to irregular shapes. Fig. 6 (b) and (c) show the FESEM images of the C/TiO_2 at calcination temperature of 300 and 700 °C, respectively. At 300 °C, FESEM image shows that the C/TiO_2 particles were non-homogeneous and agglomerated. The formation of spherical C/TiO_2 increased and became more defined as the calcination temperature increased to 700 °C.

The optical response of the C/TiO_2 and its correlation with the increasing calcination temperature was studied by DR UV-Vis spectroscopy. The UV-Vis DR spectra in the axis of Kubelka-Munk of C/TiO_2 photocatalyst calcined at 300 to 700 °C and for commercial TiO_2 are shown in Fig. 7. The figure shows a similar pattern between the C/TiO_2 and commercial TiO_2 at about 250 and 320 nm. The absorption in the range of 250 nm is associated to a charge transfer in tetrahedral-coordinated Ti between O^{2-} and the central Ti(IV) atom. The second absorption peak at 320 nm is assigned to the charge transfer in octahedral-coordinated Ti (Astorino *et al.*, 1995, Zecchina *et al.*, 1996, Nur, 2006). The absorption edges of the C/TiO_2 were remarkably shifted to higher wavelength of 360 nm when the calcination temperature increased, implying the decrease in the band gap energies from 3.54 to 3.13 eV (refer Table 1).

Fig. 8 shows the nitrogen adsorption-desorption isotherms of C/TiO_2 and commercial TiO_2. Commercial TiO_2 exhibited the Type III isotherm, characteristics of a non-porous or macroporous solid. As shown in the isotherm, the hysteresis loop in the region of P/P_0 from 0.8 to 1.0 indicates that a sorption of porous structure and an inter-particles porosity among neighbouring particles (Liu *et al.*, 2008). C/TiO_2 calcined at 300 to 600 ° showed Type IV isotherm with a H2 hysteresis loop, characteristics of a mesoporous solid, which differs from that of commercial TiO_2. At the highest calcination temperature of 700 °C, the isotherm for C/TiO_2 was identified as Type III isotherm, similar to that of commercial TiO_2. The Barret-Joyner-Halenda (BJH) pore size distribution of C/TiO_2 and commercial TiO_2 are illustrated in Fig. 9. The pore size distribution of C/TiO_2-700 and commercial TiO_2 confirmed their non-porous structures. The narrow pore size distribution curves imply that C/TiO_2 calcined at 300 to 600 °C have uniform pores in the mesopore region. The values of BET surface area, pore volume and pore diameter are presented in Table 1. It is shown that the surface area of C/TiO_2 decreased as the calcination temperature increased, from 150 to 7 m^2/g. On the other hand, when the calcination temperature increased from 300 to 600 °C, the cumulative pore volume and pore diameter of the C/TiO_2 were reduced and enlarged, respectively. The pore volume and pore diameter for C/TiO_2 composite for 700 °C and commercial TiO_2 were not available due to their non-porous structure.

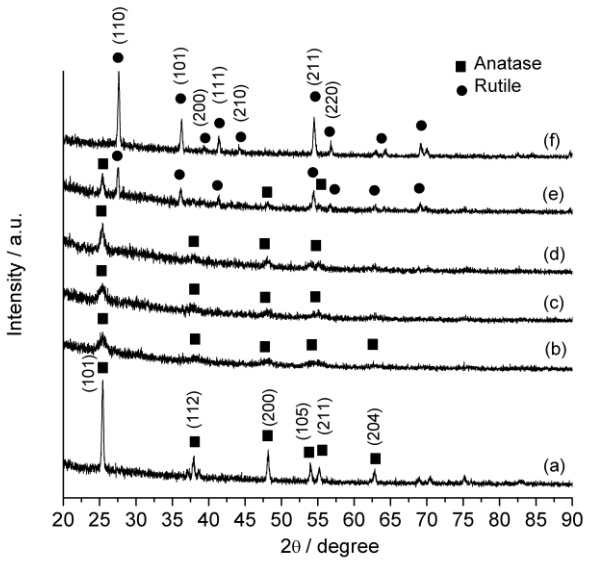

Fig. 5 XRD patterns of (a) commercial TiO_2, (b) C/TiO_2-300, (c) C/TiO_2-400, (d) C/TiO_2-500, (e) C/TiO_2-600 and (f) C/TiO_2-700

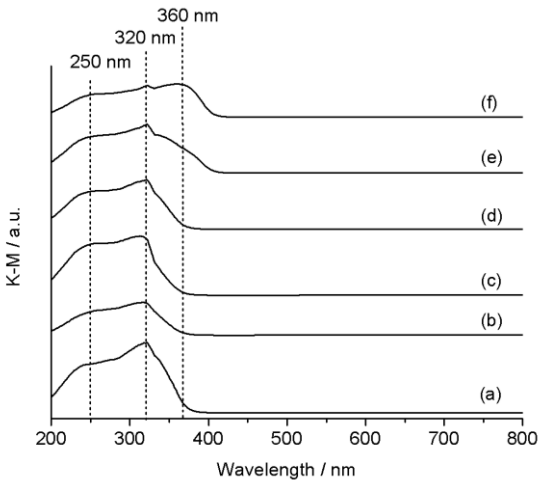

Fig. 7 DR UV-Vis spectra for (a) commercial TiO_2, (b) C/TiO_2-300, (b) C/TiO_2-400, (b) C/TiO_2-500, (b) C/TiO_2-600, (b) C/TiO_2-700.

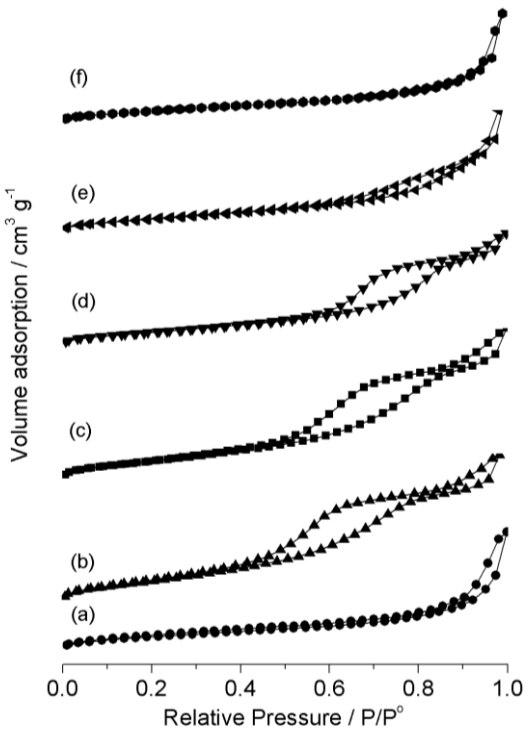

Fig. 8 Nitrogen adsorption-desorption isotherms of (a) commercial TiO_2 and C/TiO_2 samples at different calcination temperature (b) 300, (c) 400, (d) 500, (e) 600, and (f) 700 °C.

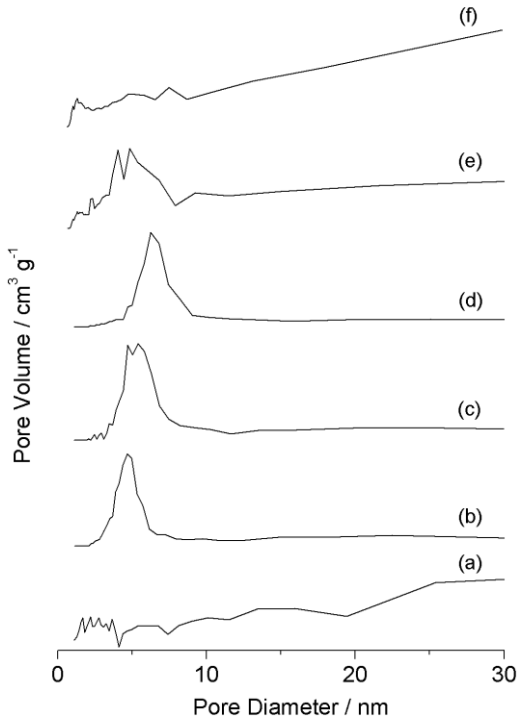

Fig. 9 Pore size distribution curve obtained from the adsorption branch of the isotherm of (a) commercial TiO_2 and (b) C/TiO_2 at different calcination temperature (b) 300, (c) 400, (d) 500, (e) 600, and (f) 700 °C

Evaluation of photocatalytic activity

The photocatalytic activity of C/TiO_2 composites were tested out in the photocatalytic oxidation of styrene under visible light irradiation. Analysis from gas chromatography indicated that benzaldehyde was the main product, alongside with styrene oxide as the minor product. The trend of photocatalytic activity in the form of yield of products' concentration is displayed in Fig. 8. As comparison, the blank experiment produced very low amount of products, as it is difficult to oxidize styrene in the absence of catalyst. However, the photo-oxidation of styrene by C/TiO_2 photocatalysts and commercial TiO_2 were significantly enhanced due to the presence of self-doped C that has been incorporated in the TiO_2's lattice which has been proven by the FTIR, XPS and EDX analyses. The Ti–C and C–O bonds from the XPS results show the presence of interstitial C-doping as well as C substitution by replacing oxygen or Ti atoms in the TiO_2 lattice. The self-doped C induced the sub band in the band gap of TiO_2 and hence, significantly enhanced the photocatalytic activity under visible light irradiation. Additionally, PL spectra also shows the presence of defect states. Hence, these characteristics allow C/TiO_2 to be an active photocatalyst under the irradiation of visible light.

The highest total concentration of products (benzaldehyde and styrene oxide) was achieved by the C/TiO_2 photocatalyst calcined at 400 and 300 °C with the concentration of 1.1 mmol and 1.0 mmol, respectively. However, when the calcination temperature of C/TiO_2 further increased to 500 - 700 °C, the yield of the products decreased. The high yield of products achieved by C/TiO_2-300 °C and C/TiO_2-400 °C could be due to the higher C content, higher surface area, and the anatase phase crystallinity. The crystal phase and crystallinity are among the most important factors for the photocatalytic activity of TiO_2, where anatase phase is considered as the most active form of TiO_2, while rutile and amorphous TiO_2 are believed to be relatively inactive (Lettmann *et al.*, 2001). Apart from that, it is known that large surface area helps to improve the photocatalytic activity of TiO_2. Surface area is correlated to the number of effective active sites, where larger surface area means more active sites, on which target molecules and intermediate products can be adsorbed. To relate the low yield of products by commercial TiO_2 to those of synthesized C/TiO_2 photocatalysts is impractical because the synthesis method of the commercial TiO_2 is unknown and it might be different from the synthesis steps of C/TiO_2 photocatalyst.

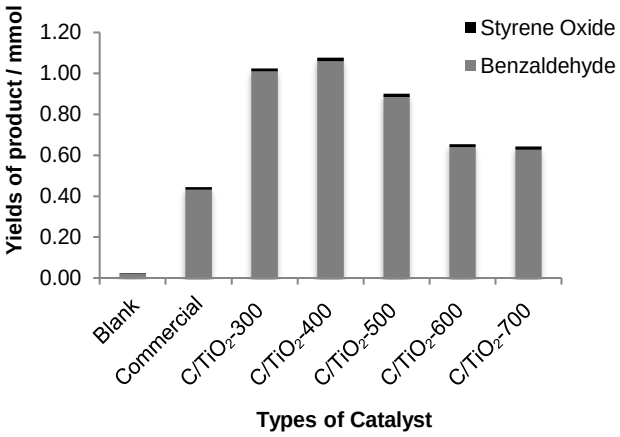

Fig. 8 Amount of products in the photo-oxidation of styrene with hydrogen peroxide under the irradiation of visible light for blank, commercial TiO_2 and the prepared C-self doped TiO_2 calcined at different temperatures, as the photocatalysts.

CONCLUSION

In this study, C self-doped TiO_2 (C/TiO_2) was synthesized using a simple sol-gel method by using titanium isopropoxide, ethanol and deionized water. Calcination temperatures of the C/TiO_2 photocatalyst affected the crystallinity, phase, morphology, surface area, porosity, crystallite size and amount of carbon present. The C/TiO_2 photocatalyst was found to be effective in oxidizing styrene under visible light irradiation due to the presence of self-doped C in the TiO_2's lattice. The self-doped C induced the sub band gap in the TiO_2 and thus enhanced the photo-oxidation under visible light irradiation. C/TiO_2-300 °C and C/TiO_2-400 °C showed high yield of products due to the higher C content, higher surface area and the anatase phase. Therefore, it is proven that TiO_2 synthesized without any external carbon source is also active for visible light photocatalytic reactions due to the presence of self-doped C.

ACKNOWLEDGEMENT

This work was financially supported by the Ministry of Science, Technology and Information, Malaysia under Fundamental Research Grant Scheme (R.J130000.7826.4F923) and Universiti Teknologi Malaysia under the Research University Grant and Ministry of Higher Education Malaysia (Vot No. 4L825 and Q.J130000.2526.18H69). One of the authors (Siti Hajar Alias) would also like to thank the Universiti Teknologi MARA Malaysia and Ministry of Higher Education Malaysia for financial support under SLAB/SLAI programme. The authors gratefully acknowlege Prof. Dr. Hadi Nur for the fruitful discussions.

REFERENCES

Astorino, E., Peri, J. B., Willey, R. J., Busca, G. 1995. Spectroscopic Characterization of silicate-1 and titanium silicate-1. *J. Catal.*, 157, 482–500.

Choi, Y., Umebayashi, T., Yoshikawa, M. 2004. Fabrication and characterization of C-doped anatase TiO_2 photocatalysts. *J. Mater. Sci.*, 39, 5, 1837–1839. doi: 10.1023/B:JMSC.0000016198.73153.31.

Ganesan, N. M., Muthukumarasamy, N., Balasundaraprabhu, R., Senthil, T. S. 2015. Importance of carbon (prepared from Azadirachta indica) for photocatalytic applications. *Optik (Stuttg).* Elsevier GmbH., 126, 22, 3317–3320. doi: 10.1016/j.ijleo.2015.07.129.

Gorska, P., Zaleska, a, Suska, a, Hupka, J. 2009. Photocatalytic Activity and Surface Properties of Carbon-Doped Titanium Dioxide. *Physicochem. Probl. Miner. Process.*, 43, 43, 21–30.

Hamal, D. B., Klabunde, K. J. 2007. Synthesis, characterization, and visible light activity of new nanoparticle photocatalysts based on silver, carbon, and sulfur-doped TiO2. *J. Colloid Interface Sci.*, 311, 2, 514–522. doi: 10.1016/j.jcis.2007.03.001.

Hanaor, D. a H., Sorrell, C. C. 2011. Review of the anatase to rutile phase transformation. *J. Mater. Sci.*, 46, 4, 855–874. doi: 10.1007/s10853-010-5113-0.

Kao, L. H., Chen, Y. P. 2017. Characterization, photoelectrochemical properties, and surface wettabilities of transparent porous TiO_2 thin films. *J. Photochem. Photobiol. A Chem.*, 340, 109–119. doi: 10.1016/j.jphotochem.2017.03.011.

Kavitha, R., Devi, L. G. 2014. Synergistic effect between carbon dopant in titania lattice and surface carbonaceous species for enhancing the visible light photocatalysis. *J. Environ. Chem. Eng.* Elsevier Ltd., 2, 2, 857–867. doi: 10.1016/j.jece.2014.02.016.

Kumar, M. M., Badrinarayanan, S., Sastry, M. 2000. Nanocrystalline TiO_2 studied by optical, FTIR and X-ray photoelectron spectroscopy: Correlation to presence of surface states. *Thin Solid Films*, 358, 1, 122–130. doi: 10.1016/S0040-6090(99)00722-1.

Lavand, A. B., Malghe, Y. S. 2015. Nano sized C doped TiO_2 as a visible light photocatalyst for the degradation of 2,4,6- trichlorophenol. *Adv. Mater. Lett.*, 6, 8, 695–700. doi: 10.5185/amlett.2015.5800.

Lettmann, C., Hildenbrand, K., Kisch, H., Macyk, W., Maier, W. F. 2001. Visible light photodegradation of 4-chlorophenol with a coke-containing titanium dioxide photocatalyst. *Appl. Catal. B Environ.*, 32, 4, 215–227. doi: 10.1016/S0926-3373(01)00141-2.

Lim, G. T., Kim, K. H., Park, J., Ohk, S. H., Kim, J. H., Cho, D. L. 2010. Synthesis of carbon-doped photocatalytic TiO_2 nano-powders by AFD process. *J. Ind. Eng. Chem.* The Korean Society of Industrial and Engineering Chemistry, 16, 5, 723–727. doi: 10.1016/j.jiec.2010.07.012.

Liu, G., Han, C., Pelaez, M., Zhu, D., Liao, S., Likodimos, V., Ioannidis, N., Kontos, A. G., Falaras, P., Dunlop, P. S. M., Byrne, J. A., Dionysiou, D. D. 2012. Synthesis, characterization and photocatalytic evaluation of visible light activated C-doped TiO_2 nanoparticles. *Nanotechnology*, 23, 29, 294003. doi: 10.1088/0957-4484/23/29/294003.

Liu, J., Zhang, Q., Yang, J., Ma, H., Tade, M. O., Wang, S., Liu, J. 2014. Facile synthesis of carbon-doped mesoporous anatase TiO_2 for the enhanced visible-light driven photocatalysis. *Chem. Commun.* Royal Society of Chemistry, 50, 13971–13974. doi: 10.1039/C4CC05544F.

Liu, Y., Zhao, W., Zhang, X. 2008. Soft template synthesis of mesoporous $Co_3O_4/RuO_2.xH_2O$ composites for electrochemical capacitors. *Electrochim. Acta 53*, 53, 3296–3304. doi: 10.1016/j.electacta.2007.11.022.

Luna, M. D. G. de, Lin, J. C.-T., Gotostos, M. J. N., Lu, M.-C. 2016. Photocatalytic oxidation of acetaminophen using carbon self-doped titanium dioxide. *Sustain. Environ. Res.* Elsevier Ltd, 26, 4, 161–167. doi: 10.1016/j.serj.2016.02.001.

Muniandy, L., Adam, F., Mohamed, A. R., Ng, E. P., Rahman, N. R. A. 2016. Carbon modified anatase TiO_2 for the rapid photo degradation of methylene blue: A comparative study. *Surfaces and Interfaces* Elsevier B.V., 5, 19–29. doi: 10.1016/j.surfin.2016.08.006.

Nur, H. 2006. Modification of titanium surface species of titania by attachment of silica nanoparticles. *Mater. Sci. Eng. B*, 133, 49–54. doi: 10.1016/j.mseb.2006.05.003.

Parayil, S. K., Kibombo, H. S., Wu, C.-M., Peng, R., Baltrusaitis, J., Koodali, R. T. 2012. Enhanced photocatalytic water splitting activity of carbon-modified TiO2 composite materials synthesized by a green synthetic approach. *Int. J. Hydrogen Energy* Elsevier Ltd, 37, 10, 8257–8267. doi: 10.1016/j.ijhydene.2012.02.067.

Park, J.-W., Kim, D.-W., Seon, H.-S., Kim, K.-S., Park, D.-W. 2010. Synthesis of carbon-doped TiO_2 nanoparticles using CO_2 decomposition by thermal plasma. *Thin Solid Films* Elsevier B.V., 518, 15, 4113–4116. doi: 10.1016/j.tsf.2009.11.013.

Park, Y., Kim, W., Park, H., Tachikawa, T., Majima, T., Choi, W. 2009. Carbon-doped TiO_2 photocatalyst synthesized without using an external carbon precursor and the visible light activity. *Appl. Catal. B Environ.*, 91, 355–361. doi: 10.1016/j.apcatb.2009.06.001.

Raja, K. S., Misra, M., Mahajan, V. K., Gandhi, T., Pillai, P., Mohapatra, S. K. 2006. Photo-electrochemical hydrogen generation using band-gap modified nanotubular titanium oxide in solar light. *J. Power Sources*, 161, 2, 1450–1457. doi: 10.1016/j.jpowsour.2006.06.044.

Shao, G. S., Liu, L., Ma, T. Y., Wang, F. Y., Ren, T. Z., Yuan, Z. Y. 2010. Synthesis and characterization of carbon-modified titania photocatalysts with a hierarchical meso-/macroporous structure. *Chem. Eng. J.* Elsevier B.V., 160, 1, 370–377. doi: 10.1016/j.cej.2010.03.011.

Simonsen, M. E., Søgaard, E. G. 2010. Sol-gel reactions of titanium alkoxides and water : influence of pH and alkoxy group on cluster formation and properties of the resulting products. *J. Sol-Gel Sci. Technol.*, 53, 485–497. doi: 10.1007/s10971-009-2121-0.

Siti Hajar Alias 2019. *Structure-photocatalytic activity relationship of carbon doped titanium dioxide analyzed by density functional theory and fuzzy logic graph*. Unpublished Doctoral Thesis. Universiti Teknlogi Malaysia, Johor, Malaysia.

Yang, X., Cao, C., Erickson, L., Hohn, K., Maghirang, R., Klabunde, K. 2008. Synthesis of visible-light-active TiO_2-based photocatalysts by carbon and nitrogen doping. *J. Catal.* Elsevier Inc., 260, 1, 128–133. doi: 10.1016/j.jcat.2008.09.016.

Zecchina, A., Bordiga, S., Lamberti, C., Ricchiardi, G., Lamberti, C., Ricchiardi, G., Scarano, D., Petrini, G., Leofanti, G., Mantegazza, M. 1996. Structural characterization of Ti centres in Ti-silicalite and reaction mechanisms in cyclohexanone ammoximation. *Catal. Today*, 32, 97–106.